Benzodioxoles: Novel Cannabinoid-1 Receptor Inverse Agonists for the Treatment of Obesity

Leo Alig, Jochem Alsenz, Mirjana Andjelkovic, Stefanie Bendels, Agnès Bénardeau, Konrad Bleicher, Anne Bourson, Pascale David-Pierson, Wolfgang Guba, Stefan Hildbrand, Dagmar Kube, Thomas Lübbers, Alexander V. Mayweg, Robert Narquizian, Werner Neidhart, Matthias Nettekoven, Jean-Marc Plancher,* Cynthia Rocha, Mark Rogers-Evans, Stephan Röver, Gisbert Schneider, Sven Taylor, and Pius Waldmeier

F. Hoffmann-La Roche Ltd, Pharmaceuticals Division, B092/4.18C, CH-4070 Basel, Switzerland

Received November 29, 2007

The application of the evolutionary fragment-based de novo design tool TOPology Assigning System (TOPAS), starting from a known CB1R (CB-1 receptor) ligand, followed by further refinement principles, including pharmacophore compliance, chemical tractability, and drug likeness, allowed the identification of benzodioxoles as a novel CB1R inverse agonist series. Extensive multidimensional optimization was rewarded by the identification of promising lead compounds, showing in vivo activity. These compounds reversed the CP-55940-induced hypothermia in Naval Medical Research Institute (NMRI) mice and reduced body-weight gain, as well as fat mass, in diet-induced obese Sprague−Dawley rats. Herein, we disclose the tools and strategies that were employed for rapid hit identification, synthesis and generation of structure−activity relationships, ultimately leading to the identification of (+)-[(*R*)-2-(2,4-dichloride-phenyl)-6-fluoro-2-(4-fluoro-phenyl)-benzo[1,3]dioxol-5-yl]-morpholin-4-yl-methanone (*R*)-14g. Biochemical, pharmacokinetic, and pharmacodynamic characteristics of (*R*)-14g are discussed.

Introduction

Scale of the Problem. Presently, the obesity epidemic represents a significant healthcare burden. As a result of the massive expansion in the prevalence of obesity in almost all societies, the World Health Organization officially declared, 10 years ago, human obesity to be one of the most significant health problems that mankind is facing.[1] In the United States, for example, the prevalence of obesity tripled during the last 25 years.[2] Such an obesity pandemic may potentially lead to a decline of life expectancy in the 21st century.[3]

Obesity is indeed a major risk factor in the development of associated diseases such as hypertension, hyperglycemia, dyslipidemia, coronary artery disease, and cancer.[4,5] The total cost in the United States for all obesity-related health problems exceeds $200 billion. More alarmingly, each year, 300 000 people die prematurely in the United States from obesity-related complications. Consequently, a tremendous need for efficient therapies to combat obesity and its associated comorbidities exists. The two main causes for the global rise in prevalence of obesity are increasingly sedentary lifestyles and high-fat, energy-rich diets.

Although lifestyle modifications may be the preferred approach for the treatment of obesity, patients often find diet and exercise insufficient or unsustainable. The first generation of centrally mediated antiobesity treatments either act by promoting neuroreceptor release and/or inhibiting reuptake mechanisms or act directly on neurotransmitter receptors.[6,7] However, these drugs have had limited success mainly for two reasons:

(1) The discrepancy between patient expectations of up to 30% body-weight loss in the first year, possibly without diet, and current therapy performance, typically 5−10% body-weight loss over the same period of time, with specific diet (compared to a placebo group under the same diet), is hampering patient compliance.

(2) Several side-effects arise either from the mechanism of action itself or from a lack of selectivity, or both.

These facts highlight the shortcoming of current therapies and the need for safer and more effective treatments of obesity, possibly as an add-on to existing therapies.

The Cannabinoid-1 Receptor and Food Intake. Among the constellation of pharmacological effects due to hashish consumption are the alteration of taste and appetite, which were already reported in 1845 and scientifically investigated in 1970.[8] Several experimental studies have shown that **3** ((−)-Δ⁹-tetrahydrocannabinol) (see Figure 1), the psycho-active constituent of marijuana, as well as endocannabinoids such as **2** (2-arachidonoyl glycerol) stimulate appetite and food intake in animal models.[9,10]

Furthermore, cannabinoid-1 receptor (CB1R)[a] subtype knockout mice resulted in markedly lower daily food intake and body weight in mice, even when they were fed with high-fat diet (HFD).[11]

These findings suggested the involvement of the endocannabinoid system in the neuronal pathway controlling appetite, food intake, and ultimately body weight. The CB1R is constitutively active, and therefore, most of the antagonists are appropriately classified as inverse agonist.[12]

In the past 10 years, several CB1R antagonist/inverse agonists including **5** (SR141716A),[13,14] **6** (SLV319),[15] and **7** (MK-0364)[16,17] have been reported to be efficacious in various animal models

---

* To whom correspondence should be addressed. Tel: 41 61 68 86 725. Fax: 41 61 68 88 714. E-mail: jean-marc.plancher@roche.com.

---

[a] Abbreviations: 5-HT₂ᵦ, 5-hydroxytryptamine 2B receptor subtype; CB1R, cannabinoid-1 receptor subtype; CB2R, cannabinoid-2 receptor subtype; DIO, diet-induced obesity; DMF, *N*,*N*-dimethylformamide; FBS: fetal bovine serum; Fassif, fasted state simulated intestinal fluid; Fessif, fed state simulated intestinal fluid; IBMX, 3-isobutyl-1-methylxanthine; h, human; HFD, high-fat diet; HRMS, high-resolution mass spectrum; LYSA, lyophilization solubility assay; MAB, maximum achievable bioavailability; MEM, modified Eagle's medium; MRI, magnetic resonance imaging; NADPH, reduced nicotinamide adenine dinucleotide phosphate; NMR, nuclear magnetic resonance; NMRI, Naval Medical Research Institute; PBS, phosphate buffered saline; SAR, structure−activity relationship; THF, tetrahydrofuran; TOPAS, topology assigning system.
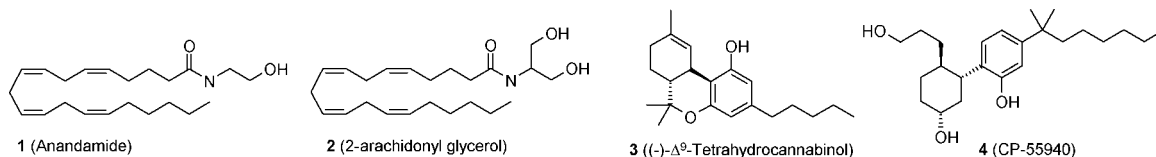
Figure 1. Some endogenous, natural and synthetic CB1R agonists.
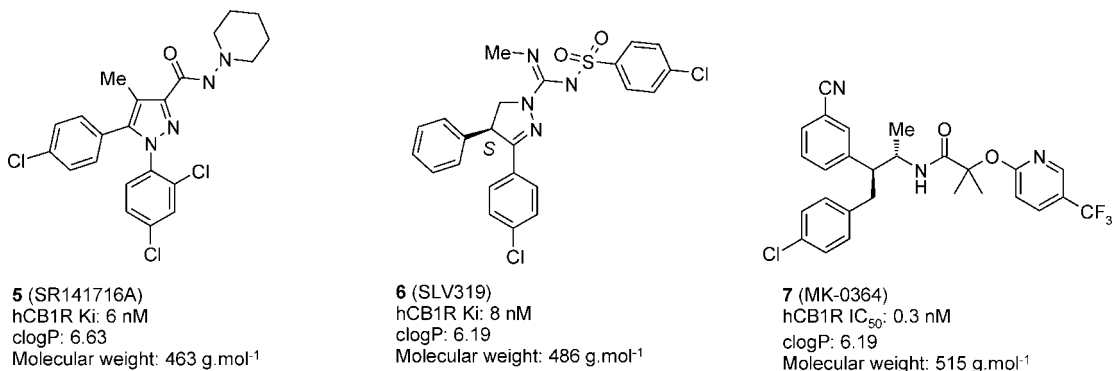
Figure 2. Selected CB1R antagonists/inverse agonists.

**Scheme 1.** Preparation of 5-*H* Phenyl Amides and Sulfonamides[a]
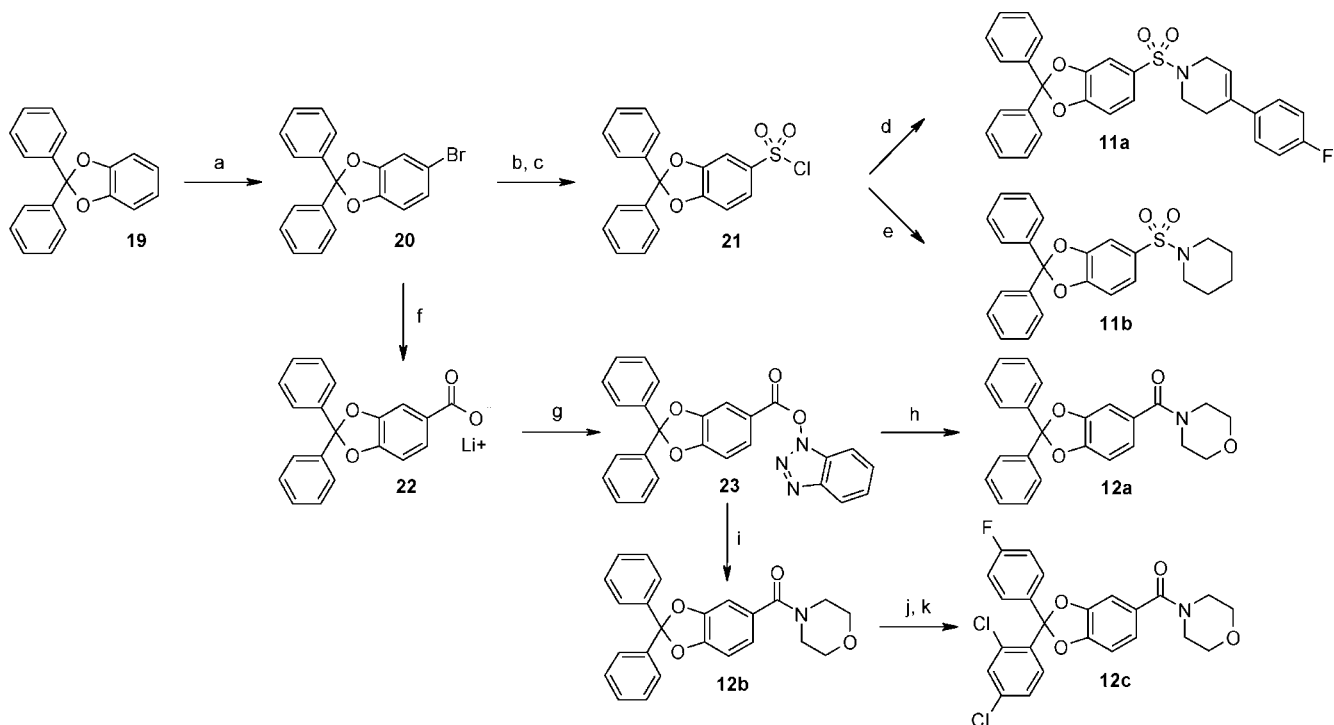
[a] Reagents and conditions: (a) *N*-bromosuccinimide, chloroform; (b) *n*-BuLi, Et₂O, then SO₂ (*g*); (c) *N*-chlorosuccinimide, chloroform; (d) iPr₂NEt, 4-(4-fluorophenyl)-1,2,3,6-tetrahydropyridine hydrochloride, dichloromethane; (e) *t*BuOK, tetrahydrofuran (THF), piperidine; (f) *n*-BuLi, THF, then CO₂ (*s*); (g) *O*-(benzotriazol-1-yl)-*N*,*N*,*N*′,*N*′-tetramethyluronium hexafluorophosphate, *N*,*N*-dimethylformamide (DMF); (h) piperidine, acetonitrile, rt; (i) morpholine, acetonitrile, rt; (j) trifluoroacetic acid, triethylsilane, rt; (k) **18b**, neat, 180 °C.

of obesity and later in patients (see Figure 2). **7** is currently undergoing phase III clinical trials for obesity and is also under evaluation as an aid for smoking cessation, whereas **5** has been approved in the European Union for the treatment of obesity.[18] However, the FDA Advisory Committee did not recommend approval of **5** for use in obese and overweight patients with associated risk factors, and consequently, the New Drug Application was withdrawn in the United States.[19]

Chemistry. A general synthetic route for CB1R ligand preparation is outlined in Scheme 1.

Bromination of 2,2-diphenyl-benzo[1,3]dioxole **19**[20] furnished preferentially **20**,[21,22] which was metallated and subsequently reacted with gaseous sulfur dioxide. The sulfinic acid lithium salt was subjected to oxidative chlorination leading to **21**. Reaction with various amines led to the desired 2,2-diphenyl-benzo[1,3]dioxole-5-sulfonic acid amides **11a** and **11b** (see Scheme 1).

From the common intermediate **20**, the lithiated species was reacted with solid carbon dioxide to afford the lithium carboxylate **22**, which was activated as its stable oxybenzotriazole

Scheme 2. Synthesis of Substituted Dichlorodiphenylmethane Derivatives[a]
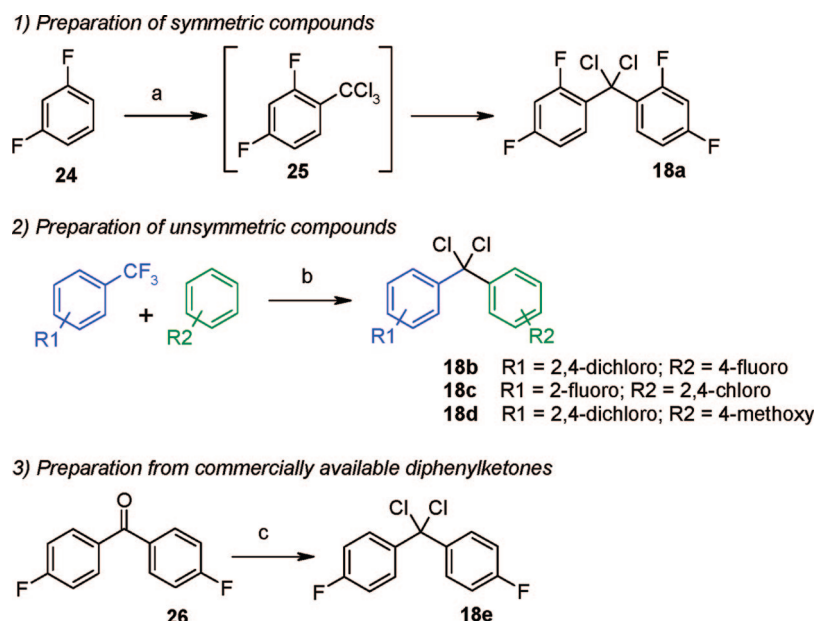
[a] Reagents and conditions: (a) tetrachloromethane, AlCl₃, 30 °C; (b) AlCl₃, 1,2-dichloroethane, 0 °C; (c) thionyl chloride, DMF, 90 °C.

derivative **23**[21,23] and subsequently reacted with several amines to afford amides **12a** and **12b**. The unsubstituted diphenylmethane motif was exchanged by hydrogenolyis and reaction with the substituted dichlorodiphenylmethane **18b**, which was prepared as shown in Scheme 2 (vide infra). Diphenyldioxomethane motifs, either used here as a catechol protecting group or as a crucial bioactive structural motif, were introduced by heating the free catechol and the dichlorodiphenylmethane without solvent at 180 °C for 20 min.[20]

Three different approaches were conveniently used to generate the required substituted dichlorodiphenylmethanes (see Scheme 2). (1) Friedel−Crafts double addition of halobenzenes onto tetrachloromethane, catalyzed by AlCl₃,[24] led quantitatively to the desired symmetrical compound **18a**, with excellent regioselectivity. (2) Friedel−Crafts alkylation of trifluoromethylbenzene derivatives with halobenzenes by using AlCl₃ afforded unsymmetrical dichlorodiphenylmethanes. Although strongly activating and *ortho*-directing substituents such as methoxy led to the desired product **18d** without detectable amount of regioisomers, fluorobenzene reacted with 2,4-dichloro-1-trifluoromethyl-benzene to give around 20% of **18c** along with the desired material **18b**. Dichlorodiphenylmethane derivatives were found to be sensitive to hydrolysis and were thus used without further purification. Therefore, separation of the regioisomers was completed at the following ketal stage. End-products derived from **18c** (see **14l**, Table 1), obtained initially as side products, proved to be biologically interesting, and **18c** was obtained regioselectively by using 2-fluoro-1-trifluoromethyl-benzene and 2,4-dichlorobenzene in the Friedel−Crafts alkylation step. (3) Alternatively, when a substituted diphenylketone was commercially available, SOCl₂-mediated chlorination was the method of choice to prepare the corresponding dichlorodiphenylmethanes.

4,5-Dihydroxy-pyridine-2-carboxylic acid **27** was obtained from kojic acid by known procedures (see Scheme 3).[25,26] The routinely applied neat process for the ketal formation, involving gaseous HCl release, led to very poor yield, and the desired product **13** was found unstable on silica gel. Although it was postulated that such unstability, even in weakly acidic media (data not shown), might be due to the protonation of the pyridine

ring, the use of potassium carbonate during the ketal formation did not lead to better yield.
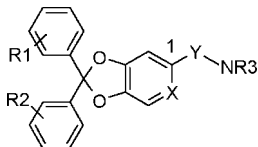
Starting from common building block **29**, a modular synthetic scheme was developed for the preparation of the 5-fluoro-phenyl amide **14a−l** and sulfonamide subseries **15a−c** (see Scheme 4). Demethylation of 4-fluoroveratrole **29** with BBr₃, followed by selective bromination of the catechol, led to **30**, which was protected with dichlorodiphenylmethane under neat conditions. Bromine−lithium exchange of **31**, facilitated by the presence of the *ortho*-fluorine, offered the possibility to use either solid carbon dioxide or chlorocarbamoyl derivatives as the electrophile to afford the carboxylic acid or amides in good yields. Compounds **14a** and **14b** were further refined by the exchange of the diphenylmethane region (see Scheme 4), allowing structure−activity relationship (SAR) exploration of the left-hand part. Reduction of the amide **14k** to amine **16** was achieved under standard reduction conditions.

Capitalizing on the orthogonal reactivity of the left and right sides of the benzodioxoles, early introduction of a functionalized ketal motif, followed by metalation of **32**, allowed late stage derivatization of the right-hand moiety, including amides **14c−l** and sulfonamides **15c**.

Alternatively, direct sulfonylation, followed by chlorination[27] of the fluoroveratrole **29**, leading to **34**, shortened the synthesis of sulfonamides from six to four linear chemical steps.

Investigation on the critical 6-position (benzodioxole numbering) was accomplished by oxidation of 6-chloropiperonal **36**[28] and reaction of the activated acid with morpholine, yielding compound **37** (see Scheme 5). Reaction with BCl₃ unlocked the catechol functionality, which was further reacted with dichlorodiphenylmethane under standard conditions to afford **17a**.

In turn, 4-methyl catechol **38** proved to be a versatile reagent, allowing the introduction of various substituents on the 6-position. Thus, selective bromination and protection afforded **39**. The 6-methyl derivative **17d** was obtained through metalation of the bromide, whereas oxidation of the methyl group by using potassium permanganate and subsequent activation of the resulting acid afforded **17b**, containing a bromine functionality in the 6-position which was subjected to further manipulation, for example, to introduce a 6-nitrile functionality as in **17c**.

Table 1. Activity of Benzodioxoles[a]

no.	R1	R2	NR3	X	Y	hCB1R K_i (nM)	hCB1R EC$_{50}$ (cAMP)	Cl human micros. μL/min/mg	Cl rat micros. μL/min/mg	hypothermia assay
11a	H	H	4-(4-fluoro-phenyl)-1,2,3, 6-tetrahydro-pyridine	C−H	SO$_2$	13	n.t.	n.t.	n.t.	inactive at 30 mg/kg ip
11b	H	H	piperidinyl	C−H	SO$_2$	38	n.t.	137	549	inactive at 30 mg/kg ip
12a	H	H	piperidinyl	C−H	CO	28	n.t.	53	673	inactive at 30 mg/kg ip
12b	H	H	morpholinyl	C−H	CO	50	784	n.t.	n.t.	n.t.
12c	2,4-Cl	4′-F	morpholinyl	C−H	CO	30	156	19	4	n.t.
13	H	H	piperidinyl	N	CO	5	n.t.	n.t.	n.t.	n.t.
14a	H	H	morpholinyl	C−F	CO	15	26	33	272	n.t.
14b	H	H	piperidinyl	C−F	CO	11	1.2	50	486	n.t.
14c	4-F	4′-F	piperidinyl	C−F	CO	7	72	48	81	n.t.
14d	2,4-Cl	4′-OMe	piperidinyl	C−F	CO	2	5	34	88	ID$_{50}$: 8 mg/kg po
14e	2,4-F	2′,4′-F	piperidinyl	C−F	CO	1	2	34	122	n.t.
14f	2,4-Cl	4′-F	piperidinyl	C−F	CO	4	5	31	89	n.t.
14g	2,4-Cl	4′-F	morpholinyl	C−F	CO	4	11	10	22	ID$_{50}$: 5 mg/kg po
14h	2,4-F	2′,4′-F	morpholinyl	C−F	CO	7	4	96	30	ID$_{50}$: 8 mg/kg po
14i	2,4-F	2′,4′-F	(4,4-difluoro-piperidinyl	C−F	CO	6	2	17	5	n.t.
14j	2,4-F	2′,4′-F	(2S)-hydroxymethyl-pyrrolidinyl	C−F	CO	46	466	20	46	n.t.
14k	4-F	4′-F	morpholinyl	C−F	CO	18	n.t.	n.t.	n.t.	n.t.
14l	2-F	2′,4′-Cl	morpholinyl	C−F	CO	4	2	21	123	ID$_{50}$: 6 mg/kg po
15a	2,4-Cl	4′-F	morpholinyl	C−F	SO$_2$	9	3	20	53	ID$_{50}$: 16 mg/kg po
15b	2,4-F	2′,4′-F	morpholinyl	C−F	SO$_2$	25	11	102	149	inactive at 30 mg/kg po
15c	2,4-F	2′,4′-F	4,4-difluoro-piperidinyl	C−F	SO$_2$	3	3	271	287	inactive at 30 mg/kg po
16	4-F	4′-F	morpholinyl	C−F	CH$_2$	>1000	n.t.	n.t.	n.t.	n.t.
17a	H	H	morpholinyl	C−Cl	CO	216	n.t.	44	388	n.t.
17b	H	H	morpholinyl	C−Br	CO	873	n.t.	n.t.	n.t.	n.t.
17c	H	H	morpholinyl	C−CN	CO	277	n.t.	n.t.	n.t.	n.t.
17d	H	H	morpholinyl	C−Me	CO	509	n.t.	n.t.	n.t.	n.t.

[a] K_i and EC$_{50}$ were calculated from dose−response curves. n.t.: not tested.

Scheme 3. Synthesis of 4,5-Dihydroxy-pyridine-2-carboxylic Acid Derivative[a]
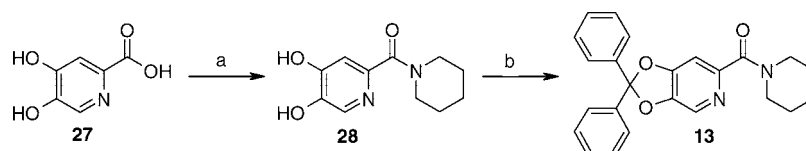
[a] Reagents and conditions: (a) 1,1′-carbonyldiimidazole, piperidine, DMF, 90 °C; (b) dichlorodiphenylmethane, potassium carbonate, DMF, 110 °C.

Those compounds presenting a stereocenter and having an interesting in vitro profile were routinely resolved by using preparative chiral HPLC. Attempts to circumvent the chromatographic purification of racemic **14g** by crystallization were unsuccessful because no crystals of **(S)-** or **(R)-14g** could be obtained. In contrast, the precursor bromoacetal **32c** was a highly crystalline compound and suitable for X-ray crystallography (see Scheme 6). Therefore, the intermediate **32c** was resolved by using chiral HPLC and **(R)-32c** was crystallized in a methanol/water solution. X-ray diffraction of this single crystal unambiguously attributed the absolute configuration as being (R). **(R)-32c** was converted in a single step to **(S)-14g** with complete retention of the configuration. Comparison of the retention time in analytical chiral HPLC of this compound with the two previously obtained enantiomers of **14g** allowed for the attribution of their absolute configurations (specific rotation at 20 °C: $^{589}\alpha = +7.33$ for **(R)-14g** and $^{589}\alpha = -6.62$ for **(S)-14g**). **(R)-14g** was confirmed as being the bioactive stereoisomer (vide infra).

Results and Discussion

Lead Identification. Our aim in this already crowded field was to rapidly identify novel CB1R ligands by making use of the evolutionary fragment-based de novo design tool TOPAS.[29,30] In a first step, the TOPAS' algorithm generated molecular fragments out of 1381 known GPCR modulators by using a computer-based retro-synthesis fragmentation scheme. In a second step, these fragments were reassembled in silico to molecular structures which are enriched with GPCR ligand motifs. These virtual compounds were ranked on the basis of their topological pharmacophore similarity to the seed molecule (see Figure 3).

The selection of the seed structure was particularly critical for this effort. Compound **8**, derived from the pyrrole series described by Huffman and co-workers,[31] was selected among others as a seed on the basis of its affinity (hCB1R $K_i = 110$ nM), rigidity, comparatively low lipophilicity (as described by clog $P = 5.68$), and molecular weight (420 g·mol^{-1}).

In addition to the predicted similarity to the seed, other parameters (including chemical tractability and patentability) were used to further bias the output generated by using the TOPAS system. From this exercise, design **9** attracted our attention and was explored. Of the nine closely related series which were investigated, only **10** retained significant affinity to the receptor (hCB1R $K_i = 1.5\ \mu$M). Hit evolution, supported

Scheme 4. Preparation of 5-Fluoro-phenyl Derivatives[a]
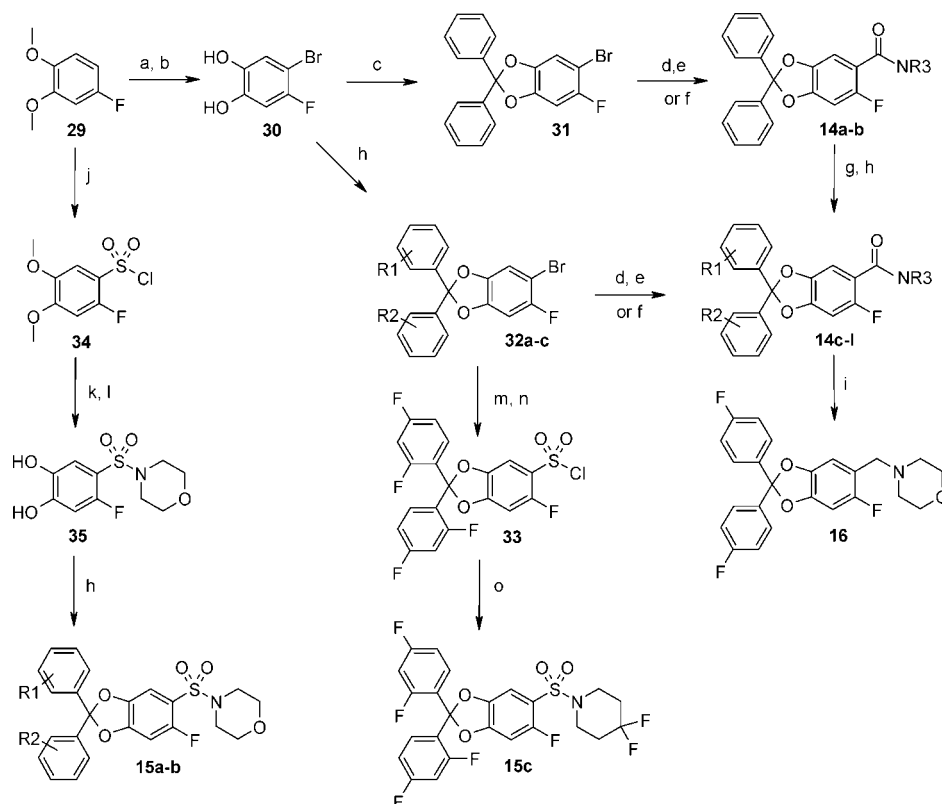
[a] Reagents and conditions: (a) BBr₃, dichloromethane, −78 to 0 °C; (b) Br₂, tetrachloromethane/chloroform/dichloromethane, rt; (c) dichlorodiphenylmethane, neat, 180 °C; (d) n-BuLi, then CO₂ (s), Et₂O, −78 °C to rt; (e) 1,1′-carbonyldiimidazole, HNR3, DMF, rt then 90 °C; (f) n-BuLi, then chlorocarbonylamine, Et₂O, −78 °C to rt; (g) trifluoroacetic acid, triethylsilane, 0 °C to rt; (h) **18a−e**, neat, 180 °C; (i) LiAlH₄, THF, rt; (j) SO₃, DMF, 1,2-dichloroethane, 85 °C, then SOCl₂, 85 °C; (k) HNR3, dichloromethane or Et₂O, rt; (l) BBr₃, dichloromethane, 0 °C to rt; (m) n-BuLi, then SO₂ (g), Et₂O, −78 to rt; (n) N-chlorosuccinimide, chloroform, rt; (o) 4,4-difluoropiperidine, Et₂O, rt.

by a pharmacophore model and rapid parallel synthesis, led to a second hit structure **11a**.[32] Remarkably, only four months were needed from the seed selection to the hit identification (see Figure 4).

Although compound **11a** complied with our needs in terms of novelty, affinity (hCB1R K_i = 13 nM), and selectivity (hCB2R K_i > 10 μM), the molecular weight and lipophilicity were still rather high for a hit compound (MW = 514 g·mol⁻¹, clog P = 7.27).

Lead Optimization: Biochemistry. Molecular modeling of **11a** and known CB1 ligands revealed that the para-fluorophenyl residue was not essential for binding and was therefore stripped off with a modest loss of binding affinity (see Figure 5, **11b**).

Replacing the sulfonyl linker (e.g., **11b**, hCB1R K_i = 38 nM) by a carbonyl linker (e.g., **12a**, hCB1R K_i = 28 nM), in spite of expected major conformational changes, helped restore the binding affinity. In contrast, reduction of the amide to the amine (see **16** vs. **14k**, Table 1) led to a dramatic loss of affinity (>1 μM).

Exchanging the phenyl central core by a pyridinyl (see **13**, Table 1), with the expectation to reduce the lipophilicity, led to an improvement in terms of binding affinity and solubility, assessed by the lyophilisation solubility assay (LYSA = 64 mg/L at pH = 6.5 in aqueous buffer). However, the poor chemical stability of **13** in weakly acid media prevented further investigations within this subseries. Replacement of the pyridinyl by fluorophenyl (see **14a**, Table 1) led to systematic and significant affinity and potency improvements (see **14a** vs **12b** and **14g** vs **12c**, Table 1). Investigations around the 6-position (see **12b**, **14a**, and **17a−d**, Table 1) rapidly
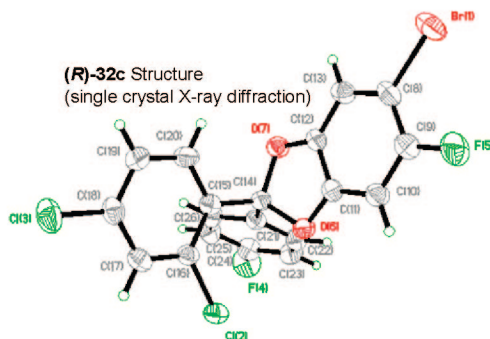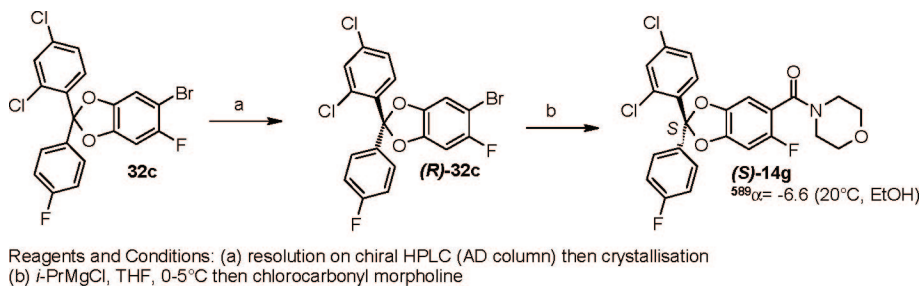
demonstrated that fluorine was optimal for binding affinity as well as for functional activation as inverse agonist, although its effect in improving metabolic stability was less pronounced (see **14g** vs **12c**, Table 1).

Diphenylmethyleneketals are known as protecting groups for catechols and can be cleaved by acidic hydrolysis.[33] To minimize such hydrolysis occurring in our CB1R inverse agonists, either during their preparation or more critically in biological fluids, most of the optimization on the phenyl ketal motif was focused on electron-withdrawing groups: among these, mainly fluorine and chlorine were introduced, and similar substitution patterns occurred on the aryl ring decoration of the **5** series. Symmetric 4,4′-difluoro substitution (see **14c**) vastly improved metabolic stability in rat microsomal preparation, most probably by shielding the metabolically sensitive *para*-position. Furthermore, an optimization of the lipophilic interactions in the CB1R binding pocket was achieved by the addition of chlorine in the 2- and 4-positions.

Lead Optimization: Biology and Physicochemistry. Application of a CB1R agonist (e.g. **4**/CP-55940, see Figure 1) in mice led to a rapid reduction of body temperature (hypothermia).[34] This reduction in body temperature was antagonized with a CB1R antagonist/inverse agonist, although the application of our CB1R antagonists/inverse agonists alone showed no significant effect. Thus, in vivo first-line screening was based on the antagonist/inverse agonist reversion of the hypothermia induced by **4** in mice. As expected from microsomal stability and CB1R potency data, application of **14d** led to a significant activity in the hypothermia assay (ID₅₀ = 8 mg/kg po).

Scheme 5. 6-Position Derivatives[a,b]

Preparation of 6-chloro derivative
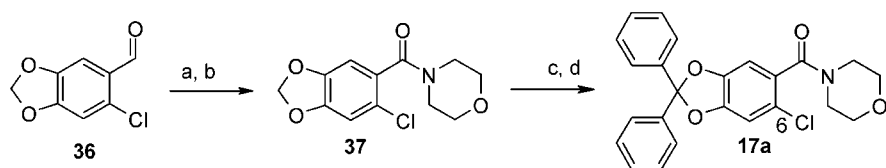
Preparation of 6-methyl, 6-bromo and 6-cyano derivatives
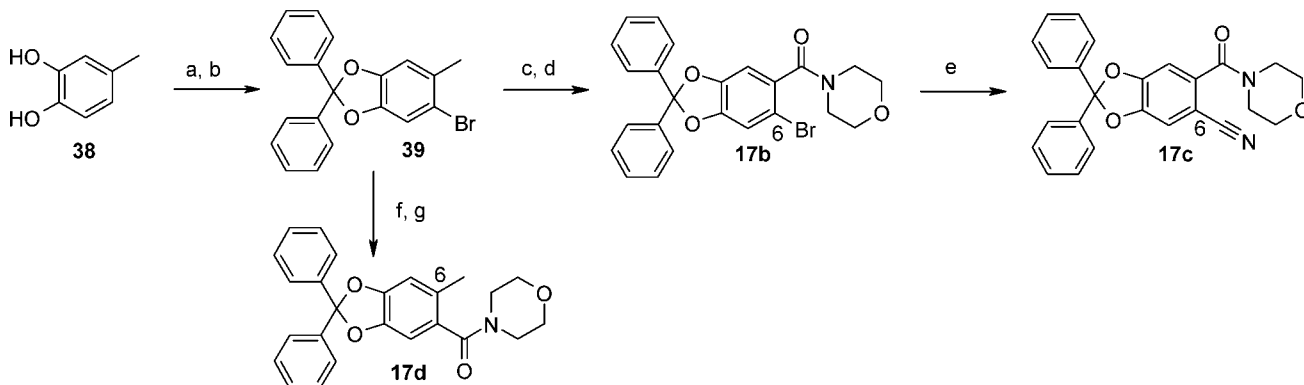
[a] Reagents and conditions for 6-chloro derivative: (a) NaClO₂, phosphoric acid, H₂O₂, acetone, H₂O, then HCl 3M; (b) 1-(2-dimethylaminopropyl)-3-ethylcarbodiimide hydrochloride, *N*-hydroxybenzotriazole, morpholine, acetonitrile, rt; (c) BCl₃, dichloromethane, 0 °C to rt; (d) dichlorodiphenylmethane, neat, 180 °C. [b] Reagents and conditions for 6-methyl, 6-bromo, and 6-cyano derivatives: (a) Br₂, dichloromethane/chloroform, rt; (b) dichlorodiphenylmethane, neat, 180 °C, 20 min; (c) KMnO₄, pyridine/water, 110 °C; (d) 1,1′-carbonyldiimidazole, DMF, morpholine, rt to 90 °C; (e) CuCN, *N*-methylpyrrolidone, 190 °C; (f) *n*-BuLi, THF, then CO₂ (*s*), −78 °C to rt; (g) *O*-(benzotriazol-1-yl)-*N,N,N′,N′*-tetramethyluronium hexafluorophosphate, morpholine, DMF, rt, 20 h.

Scheme 6. Identification of the Absolute Configuration of **14g** Enantiomers

Reagents and Conditions: (a) resolution on chiral HPLC (AD column) then crystallisation
(b) *i*-PrMgCl, THF, 0-5°C then chlorocarbonyl morpholine

(**R**)-32c Structure
(single crystal X-ray diffraction)

The water−octanol partitioning coefficient (log *D*) for most of our CB1R ligands exceeded 4 and hence our measurable window. Consequently, a calculated log *P* was routinely used to estimate lipophilicity. Plotting hCB1R binding against clog *P* revealed a correlation within several subseries, highlighting again the preference for compounds of higher lipophilicity in the receptor binding pocket. An optimization of binding affinity while closely monitoring physicochemical properties, particularly lipophilicity, was critical in our progress. Thus, binding affinity (hCB1R *K*ᵢ) was balanced against other properties, such as calculated log *P*, LYSA solubility, and microsomal clearance

(MAB: maximum achievable bioavailability, an inverse function of microsomal clearance, normalized to rat liver blood flow). Figure 6 represents a multidimensional visualization. In the bottom right quadrant, all compounds are characterized by an excellent affinity (<10 nM) but a rather poor MAB (<40%) and were therefore of limited interest. In contrast, the carbonyl-4-morpholine substituent appeared to be an interesting compromise between these four first-line screening parameters and was therefore preferentially kept in the next investigations.

Molecular modeling of the 6-fluorobenzodioxole analogue (**R**)-**14g** predicted a dihedral angle between the amide function
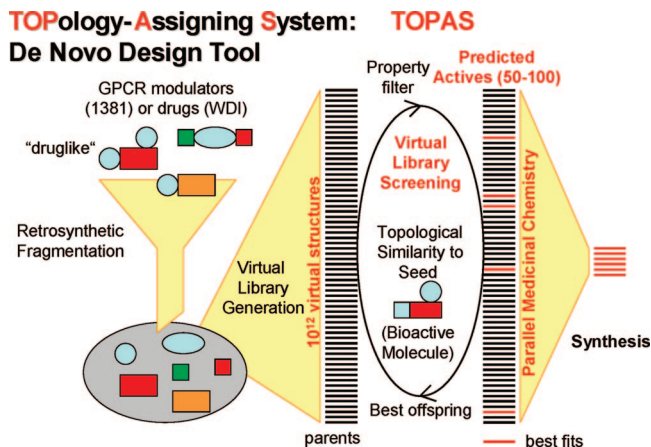
Figure 3. TOPology-Assigning System (TOPAS): Principle.

and the central aromatic ring of approximately 70°, therefore rather close to the angle estimated for the sulfonamide analogue **11b** (~90°). A re-evaluation of the sulfonamide subseries, combined with the 6-fluoro substituent, was conducted, leading indeed to potent compounds. However, metabolic stability was generally lower for the sulfonamides. Consistent with this liability is the reduced efficacy during the hypothermia assay of the sulfonamide subseries vs the amide analogues (see Table 1, **14g** vs **15a** and **14h** vs **15b**).

Characterization of (R)-14g. In the hypothermia assay, **14g** demonstrated high efficacy with an ID_{50} of 5 mg/kg po (see Table 1), even when applied in its racemic form. Resolution was performed by using chiral preparative HLPC,[35] a method which proved to be suitable up to the kilogram scale. Despite the remote stereogenic elements, the binding affinity of the enantiomer differed by about 1 logarithmic unit (hCB1R K_i = 3 nM for (R)-14g vs 35 nM for the enantiomer (S)-14g). Selectivity for the CB2R exceeded 1000-fold and was over 300-fold on a selected panel of 67 receptors, enzymes, and channels. Figure 7 shows some key characteristics of (R)-14g.

Highly representative for CB1R inverse agonists, (R)-14g is characterized by a high lipophilicity (clog P = 5.82) and, despite optimization efforts, a low solubility in aqueous media (<1 mg/L in pH = 6.5 buffer). However, solubility in fasted-state and fed-state simulated intestinal fluids (Fassif and Fessif) was considerably higher (129 and 445 mg/L, respectively). Cell membrane permeation determined in Caco2 cells led to a good apical-to-basolateral permeation (Pe = 10.6 $\times 10^{-6}$ cm/s).[36]

Oral application of (R)-14g reversed the hypothermia induced by the application of **4** with an ID_{50} of 4 mg/kg, (see Figure 8). This value was directly comparable to the performance of **5** used as a positive control.

To evaluate (R)-14g in a disease-relevant model, male Sprague–Dawley rats were fed with a HFD (43% of energy from fats) 10 weeks prior to the treatment period and during dosing. Chronic application of (R)-14g (1, 3, and 10 mg/kg) and **5** (10 mg/kg) for 16 days in this diet-induced obesity (DIO) rat model led to a slower progression of body weight in all groups, statistically significant for the 3 and 10 mg/kg groups with (R)-14g and for the 10 mg/kg group for **5** (see Figure 9). This dose-dependent body-weight reduction was associated with a reduction in body fat, measured by magnetic resonance imaging (MRI).

Conclusion

A series of benzodioxole derivatives was identified as a novel class of CB1R inverse agonists.[23,35,37,38] A chemistry starting

point was rapidly identified by using the de novo design tool TOPAS and rapid parallel synthesis. After SAR development and extensive multidimensional optimization, (R)-14g proved to have the best overall characteristics for advancement. In an indirect acute pharmacodynamic model, (R)-14g reversed dose-dependently the hypothermia induced by **4**. Furthermore, in a 16-day DIO rat model, (R)-14g demonstrated a robust reduction in body-weight gain, correlated with a reduction of food intake. In this model, (R)-14g proved to be equipotent to **5**. On the basis of its efficacy and selectivity profile, compound (R)-14g was selected for further evaluation for the treatment of obesity.

Experimental Section

Chemistry. General. Proton nuclear magnetic resonance (NMR) spectra were obtained on a Bruker 250, 300 or 400 MHz instrument with chemical shifts (δ) reported relative to tetramethylsilane as an internal standard. Elemental analyses were performed by Solvias AG (Mattenstrasse, Postfach, CH-4002 Basel). Column chromatography was carried out on silica gel 60 (32−60 mesh, 60 Å) or on prepacked columns (Isolute Flash Si). Mass spectra were recorded on SSQ 7000 (Finnigan-MAT) for electron impact ionization. High-resolution mass spectrum (HRMS) were recorded on Nanospray Bruker Reflex.

Detailed Description. 5-Bromo-2,2-diphenyl-benzo[1,3]dioxole (20). To a mixture of 2,2-diphenyl-benzo[1,3]dioxole[20] (27.4 g, 100 mmol) in chloroform (80 mL) was added N-bromosucinimide (18.75 g, 105 mmol). The reaction mixture was refluxed for 20 h, cooled, and filtered. The filtrate was washed with water, dried over sodium sulfate, and concentrated in vacuo. The residue was recrystallized from ethanol to afford the desired product as white crystals (14.15 g, 40%). ^{1}H NMR (400 MHz, DMSO-d_6) δ 7.01 (d, J = 8 Hz, 1H); 7.07 (dd, J = 8 Hz, <1 Hz, 1H); 7.30 (d, J < 1 Hz, 1H); 7.40−7.50 (m, 6H); 7.50−7.56 (m, 4H). MS (EI) m/e 352 (M$^{+•}$). mp: 88−89 °C.

1-(2,2-Diphenyl-benzo[1,3]dioxole-5-sulfonyl)-4-(4-fluoro-phenyl)-1,2,3,6-tetrahydro-pyridine (11a). To a mixture of 4-(4-fluorophenyl)-1,2,3,6-tetrahydropyridine hydrochloride (2.56 g, 12 mmol) in dichloromethane (150 mL) was added N-ethyldiisopropylamine (4.2 mL, 25 mmol), and the reaction was stirred for 10 min at room temperature. 2,2-Diphenyl-benzo[1,3]dioxole-5-sulfonyl chloride (20) (3.72 g, 10 mmol) was added, and the reaction was stirred 2 h at room temperature. The solvent was evaporated in vacuo, and the residue was purified by column chromatography on silica gel (dichloromethane as eluant). The product was crystallized from hexane to afford the desired product as white crystals (3.8g, 75%). ^{1}H NMR (300 MHz DMSO-d_6) δ 2.50 (m, 2H); 3.23 (t, J = 5.6 Hz, 2H); 3.68 (bs, 2H); 6.03 (bs, 1H); 7.09 (t, J = 8.9 Hz, 2H); 7.26 (d, J = 8.2 Hz, 1H); 7.36−7.40 (m, 3H); 7.44−7.48 (m, 7H); 7.50−7.54 (m, 4H). MS m/e (IPS) 514.3 (M + H$^+$). Anal. ($C_{30}H_{24}FNO_4S$) C, H, N, O, F, S. HRMS $C_{30}H_{24}F$-NO_4S: 514.14841 (M + H$^+$).

1-(2,2-Diphenyl-benzo[1,3]dioxole-5-sulfonyl)-piperidine (11b). To a mixture of 2,2-diphenyl-benzo[1,3]dioxole-5-sulfonyl chloride (20) (2.0 g, 5.4 mmol) and potassium tert-butoxide (840 mg, 7.5 mmol) in THF (20 mL) was added piperidine (1.17 mL, 11.8 mmol). The dark reaction mixture was stirred 20 h at room temperature and partitioned between dichloromethane and 0.5 M aqueous hydrochloric acid. The aqueous phase was extracted with dichloromethane, and the combined organic phases were washed with saturated aqueous solution of sodium hydrogencarbonate and brine, concentrated in vacuo, and purified by column chromatography on silica gel (cyclohexane/ethyl acetate 9:1 as eluant) to afford the desired product as a white solid (737 mg, 33%). ^{1}H NMR (300 MHz, CDCl$_3$) δ 1.35−1.50 (m, 2H); 1.60−1.70 (m, 4H); 2.97 (dd, J = 5.4, 5.4 Hz, 4H); 6.95 (d, J = 8.4 Hz, 1H); 7.25 (s, 1H); 7.28 (dd, J = 8.0, 0.8 Hz, 1H); 7.35−7.50 (m, 6H); 7.53−7.58 (m, 4H). MS (EI) m/e 422.2 (M + H)$^+$. Anal. ($C_{24}H_{23}NO_4S$) C, H, N, O, S. HRMS $C_{24}H_{23}NO_4S$: 422.14204 (M + H$^+$).
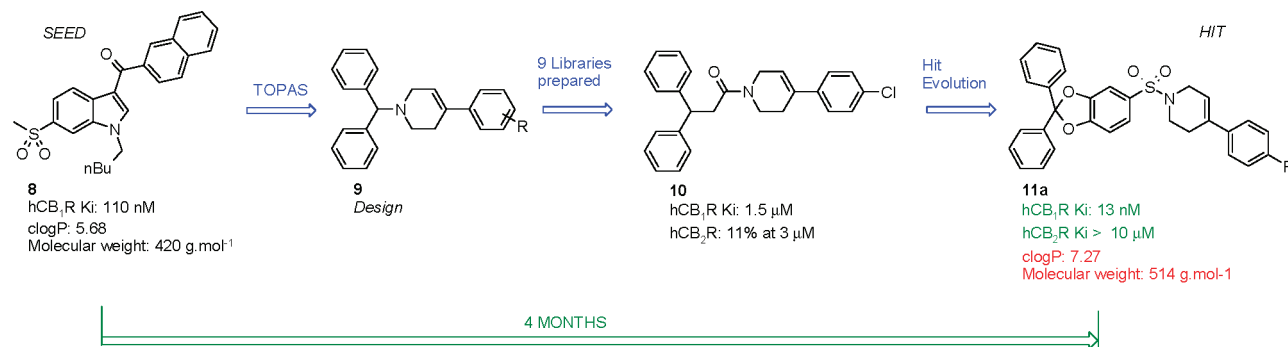
Figure 4. From seed to hit within four months by using TOPAS and rapid parallel synthesis.
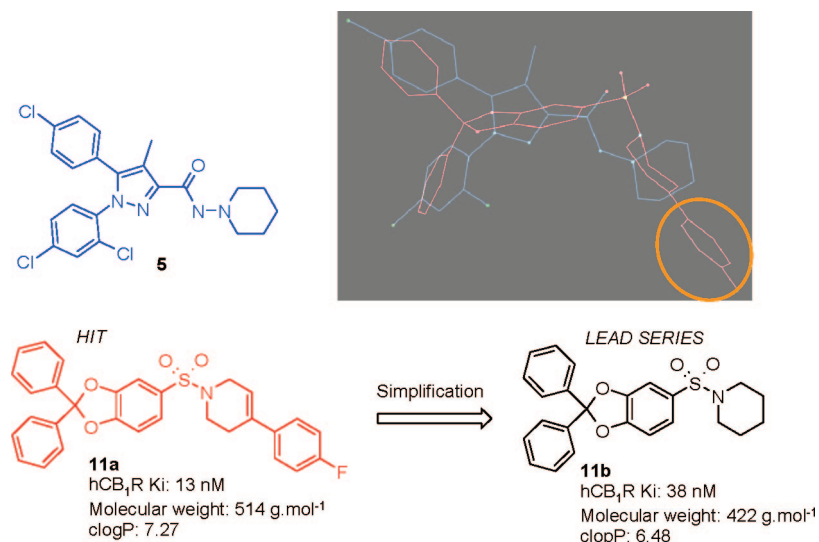

Figure 5. Modeled overlay of sulfonamide **11a** and **5**. *para*-Fluorophenyl (in the orange circle) did not appear essential.

(2,2-Diphenyl-[1,3]dioxolo[4,5-c]pyridin-6-yl)-piperidin-1-yl-methanone (13). A mixture of 4,5-dihydroxy-2-pyridinecarboxylic acid[25,26] (116 mg, 0.75 mmol) and carbonyldiimidazole (122 mg, 0.75 mmol) in DMF (5 mL) was stirred at room temperature overnight. Piperidine (75 μL, 0.75 mmol) was added, and the reaction was heated 5 h at 90 °C. After cooling, the reaction was poured onto diethyl ether. A solid precipitated. The liquid phase was decanted from the precipitated solid, and the residue was dried in vacuo to afford (4,5-Dihydroxy-pyridin-2-yl)-piperidin-1-yl-methanone **28** (110 mg, 69%) as an off-white solid which was used without further purification.

(4,5-Dihydroxy-pyridine-2-yl)-piperidin-1-yl-methanone **28** (110 mg, 0.5 mmol) was dissolved in DMF (5 mL) and heated to 100 °C. Potassium carbonate (76 mg, 0.55 mmol) and dichlorodiphenylmethane (0.1 mL, 0.55 mmol) were added, and the reaction was stirred overnight at 110 °C. After cooling, the mixture was partitioned between water (50 mL) and ethyl acetate. The aqueous phase was extracted with ethyl acetate (three times), and the combined organic phases were washed with water and brine. The solvents were removed in vacuo, and the residue was purified by column chromatography on silica gel (dichloromethane/ethyl acetate 1:0−0:1 as eluant) to afford the desired product as white wax (5 mg, 3%). ^{1}H NMR (250 MHz, DMSO-d_6) δ 1.44−1.59 (m, 6H); 3.32 (m, 2H); 3.56 (m, 2H); 7.33 (s, 1H); 7.45−7.59 (m, 10H); 8.26 (s, 1H). MS m/e (IPS) 387.3 (M + H+).

4-Fluoro-benzene-1,2-diol. To a cold (acetone/dry-ice bath) solution of boron tribromide in dichloromethane (1 M, 132 mL, 738 mmol) was added the 1-fluoro-3,4-dimethoxybenzene (34 mL, 256 mmol) over 40 min. After the addition, the reaction mixture was allowed to warm up to room temperature and was stirred for an additional 3 h. The brown reaction mixture was partioned between ice−water (1 L) and ethyl acetate (300 mL) and then extracted with ethyl acetate. The combined organic phases were washed with saturated aqueous sodium hydrogenocarbonate solution and brine. The combined organic phases were dried over sodium sulfate and evaporated in vacuo to afford the desired product as a brown oil (25 g, 46%) which was used without further purification. ^{1}H NMR (300 MHz, CDCl₃) δ 5.64 (bs, 1H); 6.09 (bs, 1H); 6.49 (ddd, J = 8.8, 8.6, 2.7 Hz, 1H); 6.64 (dd, J = 9.3, 2.7 Hz, 1H); 6.78 (dd, J = 8.8, 5.3 Hz, 1H). MS (EI) m/e 129.1 (M + H)+.

4-Bromo-5-fluoro-benzene-1,2-diol (30). To a solution of 4-fluoro-benzene-1,2-diol (25 g, 117 mmol) in chloroform (228 mL) and dichloromethane (46 mL) was added a solution of bromine (24 g, 150 mmol) in tetrachloromethane (27 mL) over 40 min. The reaction mixture was stirred 3 h at room temperature, and volatiles were evaporated in vacuo. Purification was performed by using column chromatography on silica gel (dichloromethane/ethyl acetate 19:1 as eluant) to afford the desired product as a brown oil (30 g, 92%). ^{1}H NMR (400 MHz, CDCl₃) δ 5.34 (s, 1H); 5.66 (s, 1H); 6.73 (d, J = 12 Hz, 1H); 7.01 (d, J = 8 Hz, 1H). MS (EI) m/e 207.2 (M + H)+.

5-Bromo-6-fluoro-2,2-diphenyl-benzo[1,3]dioxole (31). A mixture of 4-bromo-5-fluoro-benzene-1,2-diol **30** (102 g, 0.49 mol) and dichlorodiphenylmethane (140 g, 0.59 mol) was heated at 180 °C under a stream of nitrogen. After 20 min, the brown mixture was removed from the oil bath and allowed to cool. The residue was diluted with methanol (400 mL) under rapid stirring. The product precipitated after a few minutes. The product was filtered, dried, and recrystallized from methanol to afford the product as a light-brown solid (116.5 g, 63%). ^{1}H NMR (400 MHz, CDCl₃) δ 6.72 (d, J = 7 Hz, 1H); 7.00 (d, J = 7 Hz, 1H); 7.35−7.45 (m, 6H); 7.5−7.6 (m, 4H). MS m/e 370 (M)+.
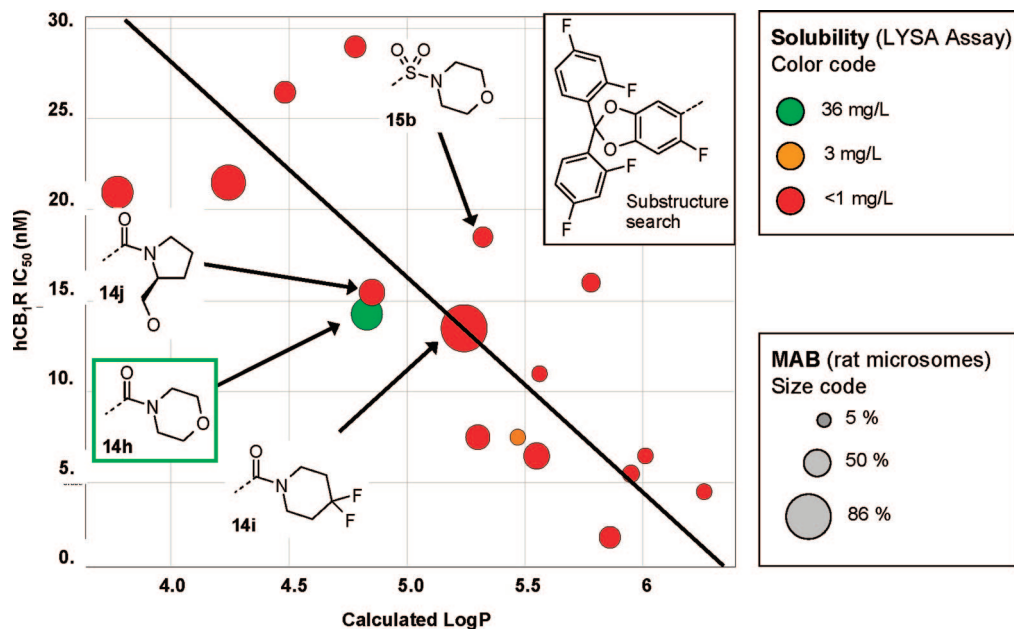
Figure 6. Multidimensional (4D) visualization. Calculated log *P* and binding affinity tend to correlate in a defined subseries, requiring a compromise with other properties, i.e., calculated log *P*, solubility in LYSA, and microsomal clearance expressed as MAB.
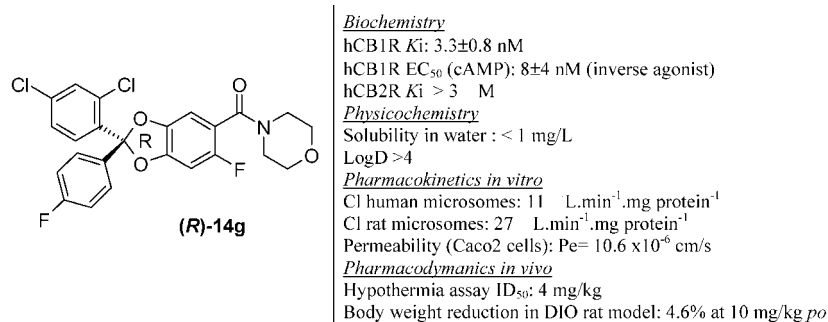

Biochemistry
hCB1R Ki: 3.3±0.8 nM
hCB1R EC$_{50}$ (cAMP): 8±4 nM (inverse agonist)
hCB2R Ki > 3 M
Physicochemistry
Solubility in water : < 1 mg/L
LogD >4
Pharmacokinetics in vitro
Cl human microsomes: 11 L.min^{-1}.mg protein^{-1}
Cl rat microsomes: 27 L.min^{-1}.mg protein^{-1}
Permeability (Caco2 cells): Pe= 10.6 x10^{-6} cm/s
Pharmacodymanics in vivo
Hypothermia assay ID$_{50}$: 4 mg/kg
Body weight reduction in DIO rat model: 4.6% at 10 mg/kg *po*

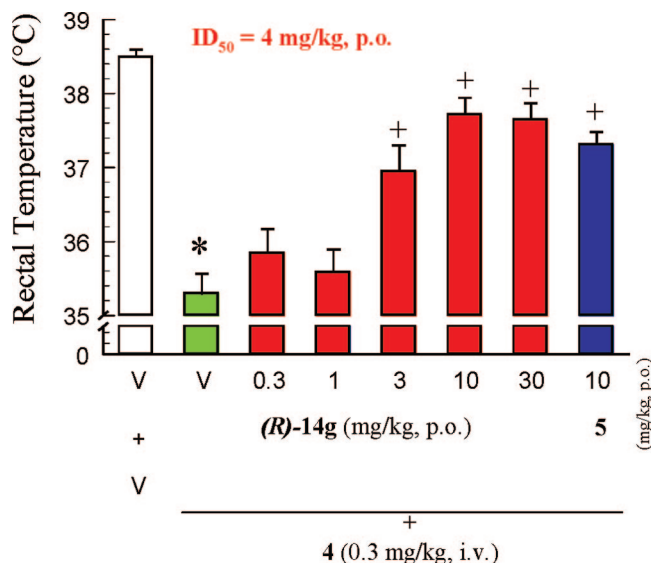**Figure 7.** Some key characteristics of (*R*)-14g.

Figure 8. Reversion of **4**-induced hypothermia in mice by using (*R*)-**14g** and **5**.

(6-Fluoro-2,2-diphenyl-benzo[1,3]dioxol-5-yl)-morpholin-4-yl-methanone (14a). To a cooled (−78 °C) solution of 5-bromo-6-fluoro-2,2-diphenyl-1,3-benzodioxole **31** (91.8 g, 247 mmol) in diethyl ether (1500 mL) was added a solution of *n*-butyl lithium in

hexane (1.6 M solution, 170 mL, 272 mmol) at a rate such that the temperature did not exceed −72 °C. The addition was completed after 30 min, and the mixture was stirred 1 h at −78 °C to afford a yellow solution. 4-Morpholinecarbonyl chloride (42.7 mL, 371 mmol) was added at a rate such that the temperature did not exceed −67 °C. A precipitate formed. The cooling mechanism was removed, and the suspension was allowed to warm by 10 °C (about 1.5 h). The reaction mixture was quenched by the addition of saturated aqueous sodium bicarbonate solution (200 mL, saturated solution), and the mixture was extracted with diethyl ether. The combined organic phases were washed with saturated sodium bicarbonate solution (300 mL) and brine (500 mL) and dried over sodium sulfate, and the solution was concentrated to ~400 mL. The product crystallized as a white solid (49.0 g, 60%). mp: 174−177 °C. ^{1}H NMR (400 MHz, CDCl$_3$) δ 3.37 (bs, 2H); 3.63 (bs, 2H); 3.75 (bs, 4H); 6.63 (d, *J* = 8.4 Hz, 1H); 6.87 (d, *J* = 5.6 Hz, 1H); 7.38 (m, 6H); 7.54 (m, 4H). MS (ISP) *m/e* 406.4 (M + H)$^+$. Anal. (C$_{24}$H$_{20}$FNO$_4$) C, H, N, O, F. HRMS C$_{24}$H$_{20}$FNO$_4$: 406.14491 (M + H$^+$).

2,4-Dichloro-1-[dichloro-(4-fluoro-phenyl)-methyl]-benzene (18b). To a cold (ice bath) suspension of aluminum trichloride (129.3 g, 0.96 mol) in 1,2-dichloroethane (450 mL) was slowly added 2,4-dichlorobenzotrifluoride (70 g, 0.32 mol) in 60 min. Fluorobenzene (30 mL, 0.32 mol) was slowly added to the dark-red mixture in 60 min. The reaction mixture was stirred 5 h at 0 °C and poured onto crushed ice. The aqueous phase was extracted with dichloromethane, and the combined organic phases were washed with water and brine, dried over sodium sulfate, and dried in vacuo to afford the desired product as a dark-yellow oil (110.4
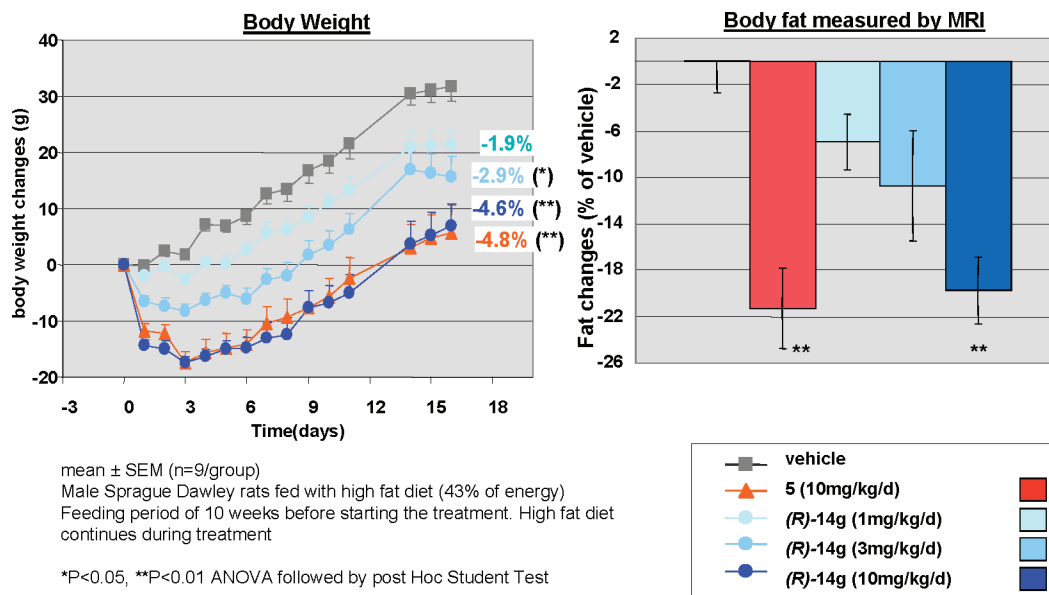
Figure 9. Chronic application of (**R**)-**14g** and **5** in a DIO rat model. Dose-dependent reduction of body weight was observed in correlation with body fat loss.

g, quantitative) which was used without further purification. ¹H NMR (300 MHz, CDCl₃) δ 7.0−7.10 (t, 2H, *J* = 8.8 Hz); 7.35−7.55 (m, 4H); 8.28 (d, *J* = 8.7 Hz, 1H). MS (EI) *m/e* 325.0 (M + H)⁺.

5-Bromo-2-(2,4-dichloro-phenyl)-6-fluoro-2-(4-fluoro-phenyl)-benzo[1,3]dioxole (32c). A mixture of 4-bromo-5-fluoro-benzene-1,2-diol **30** (15 g, 72 mmol) and 2,4-dichloro-1-[dichloro-(4-fluoro-phenyl)-methyl]-benzene **18b** (25.8 g, 80 mmol) was heated 20 min at 180 °C under a stream of nitrogen. The resulting brown mixture was purified by column chromatography on silica gel (cyclohexane/dichloromethane 1:0−19:1 as eluant) to afford the desired product as a light-yellow oil (21.1 g, 64%). ¹H NMR (300 MHz, CDCl₃) δ 6.75 (d, *J* = 5.7 Hz, 1H); 7.03−7.1 (m, 3H); 7.33 (dd, *J* = 8.4, 2.1 Hz, 1H); 7.40−7.45 (m, 3H); 7.72 (d, *J* = 8.4 Hz, 1H). MS (EI) 456, 458 (M).

(R)-5-Bromo-2,2-bis-(2,4-difluoro-phenyl)-6-fluoro-benzo[1,3]dioxole ((R)-32c). A total of 28 mg of racemic 5-bromo-2-(2,4-dichloro-phenyl)-6-fluoro-2-(4-fluoro-phenyl)-benzo[1,3]-dioxole **32c** was separated into its enantiomers by semipreparative HPLC by using an analytical Chiralpak AD-H column (250 × 4.6 mm, 5 μm) in the polar-organic mode by using MeCN/EtOH 96:4 as mobile phase (flow: 1.0 mL/min, detection at 210 nm), affording approximately 14 mg of each enantiomer. The earlier eluting enantiomer **32c** (*t*ᴿ = 4.33 min) was then dissolved in MeOH (1 mL) and treated at room temperature with water (0.1 mL). After 30 min, crystals suitable for X-ray analysis formed. The absolute configuration of this enantiomer was determined to be *R*.

2-(2,4-Dichloro-phenyl)-6-fluoro-2-(4-fluoro-phenyl)-benzo[1,3]dioxole-5-carboxylic Acid. To a cold mixture (dry ice/acetone bath) of 5-bromo-2-(2,4-dichloro-phenyl)-6-fluoro-2-(4-fluoro-phenyl)-benzo[1,3]dioxole **32c** (16.5 g, 36 mmol) in diethylether (250 mL) was slowly added a solution of *n*-butyllithium in hexane (1.6 M, 23 mL, 37 mmol). The reaction mixture was stirred 1 h at −78 °C, and solid carbon dioxide (approximately 50 g) was added to the dark solution. The reaction mixture was allowed to warm up to room temperature to form a copious precipitate. After 4 h at room temperature, the reaction mixture was partitioned between aqueous 0.5 N hydrochloric acid solution and ethyl acetate. The aqueous phase was extracted three times with ethyl acetate. The combined organic phases were concentrated in vacuo, and the residue was purified by column chromatography on silica gel (dichloromethane/methanol 19:1 as eluant) to afford the product as a yellow solid (4.48 g, 29%). ¹H NMR (300 MHz, CDCl₃) δ 6.73 (d, *J* = 9.9 Hz, 1H); 7.08 (t, *J* = 8.5 Hz, 2H); 7.33

(dd, *J* = 8.4, 2.1 Hz, 1H); 7.41−7.51 (m, 4H); 7.73 (d, *J* = 8.7 Hz, 1H). MS *m/e* (EI) 422 (M − H)⁻.

[2-(2,4-Dichloro-phenyl)-6-fluoro-2-(4-fluoro-phenyl)-benzo[1,3]dioxol-5-yl]-morpholin-4-yl-methanone (14g). A solution of 2-(2,4-dichloro-phenyl)-6-fluoro-2-(4-fluoro-phenyl)-benzo[1,3]dioxole-5-carboxylic acid (4.03 g, 9.2 mmol) and carbonyldiimidazole (1.95 g, 12.0 mmol) in DMF (60 mL) was stirred at room temperature overnight. Morpholine was added (2 mL, 23 mmol), and the reaction mixture was stirred 8 h at 90 °C. The reaction mixture was partitioned between ethyl acetate and aqueous sodium hydrogenocarbonate solution. The aqueous phase was extracted with ethyl acetate, and the combined organic phases were washed with brine, dried over sodium sulfate, filtered, and evaporated in vacuo. The residue was purified by column chromatography on silica gel (cyclohexane/ethyl acetate 1:1 as eluant) to afford the product as an off-white foam (4.24 g, 93%). ¹H NMR (300 MHz, CDCl₃) δ 3.10 (bs, 2H); 3.38 (bs, 2H); 3.38 (bs, 4H); 6.68 (d, *J* = 8.4 Hz, 1H); 6.91 (d, *J* = 5.4 Hz, 1H); 7.07 (t, *J* = 8.4 Hz, 2H); 7.32 (dd, *J* = 8.7, 2.1 Hz, 1H); 7.40−7.46 (m, 3H); 7.75 (d, *J* = 8.7 Hz, 1H). MS *m/e* (EI) 492.1 (M + H)⁺. Anal. (C₂₄H₁₇F₂Cl₂NO₄) C, H, N, O, F, Cl. HRMS C₂₄H₁₇Cl₂F₂NO₄: 492.05748 (M + H⁺).

(S) and (R) [2-(2,4-Dichloro-phenyl)-6-fluoro-2-(4-fluoro-phenyl)-benzo[1,3]dioxol-5-yl]-morpholin-4-yl-methanone ((S)- and (R)-14g). Preparative HPLC: racemic 2-(2,4-dichloro-phenyl)-6-fluoro-2-(4-fluoro-phenyl)-benzo[1,3]dioxole-5-carboxylic acid **14 g** (250 mg/run) was dissolved in ethanol/heptane (1:1, 4 mL) and injected onto a preparative chiral HPLC (column, 20 μm ChiralPak AD, Daicel Chemical Industries, Ltd.; 5 × 50 cm; flow, 35 mL/min; 15 bar; solvents, heptane/isopropanol 90:10). UV detection was performed at 225 nm.

Analytical HPLC: (column, 20 μm ChiralPak AD, Daicel Chemical Industries Ltd.; 0.46 × 25 cm; flow, 1 mL/min; 28 bar; solvents, heptane/isopropanol 90:10).

(S)-(−)-[2-(2,4-Dichloro-phenyl)-6-fluoro-2-(4-fluoro-phenyl)-benzo[1,3]dioxol-5-yl]-morpholin-4-yl-methanone ((S)-14g). Yield: 31% (off-white solid). Retention time: 240 min (preparative HPLC); 31.0 min (analytical HLPC). Enantiomeric ratio (analytical HPLC): 94%.

Specific rotation: −6.62 °·mL·g⁻¹·dm⁻¹ at 589 nm in MeOH; −37.26 °·mL·g⁻¹·dm⁻¹ at 365 nm in MeOH. Anal. (C₂₄H₁₇-F₂Cl₂NO₄) calc. C = 58.55%, H = 3.48%, N = 2.85%, O =13.00%, F = 7.72%, Cl = 14.40%; found: C = 58.25%, H = 3.56%, N = 3.07%, O = 13.43%, F = 7.72%, Cl = 14.04%. HRMS C₂₄H₁₇Cl₂F₂NO₄: 492.05761 (M + H⁺).

(R)-(−)-[2-(2,4-Dichloro-phenyl)-6-fluoro-2-(4-fluoro-phenyl)-benzo[1,3]dioxol-5-yl]-morpholin-4-yl-methanone ((R)-14g). Yield: 43% (off-white solid). Retention time: 295 min (preparative HPLC); 35.0 min (analytic HLPC). Enantiomeric ratio (analytical HPLC): 99%. Specific rotation: +7.33 $°\cdot mL\cdot g^{-1}\cdot dm^{-1}$ at 589 nm in MeOH; +41.83 $°\cdot mL\cdot g^{-1}\cdot dm^{-1}$ at 365 nm in MeOH. Anal. ($C_{24}H_{17}F_2Cl_2NO_4$) C, H, N, O, F, Cl. HRMS $C_{24}H_{17}Cl_2F_2NO_4$: 492.05759 (M + H$^+$).

(S)-[2-(2,4-Dichloro-phenyl)-6-fluoro-2-(4-fluoro-phenyl)-benzo[1,3]dioxol-5-yl]-morpholin-4-yl-methanone ((S)-14g). A solution of (R)-5-bromo-2,2-bis-(2,4-difluoro-phenyl)-6-fluoro-benzo[1,3]dioxole (R)-32c (2.0 mg, 4.4 μmol) in THF (16 μL) was treated at 0−5 °C with a solution of isopropyl magnesium chloride in THF (2 M, 22 μL, 44 μmol), and the resulting mixture was stirred 1 h at 0 °C. To the clear solution was added 4-morpholine carbonyl chloride (10.3 μL, 88 μmol). The reaction mixture was diluted with THF (2 mL) and quenched with water (100 μL). The resulting mixture was dried over MgSO$_4$ and evaporated in vacuo. The residue was purified by column chromatography on silica gel (1 g silica gel, heptane/ethyl acetate 10:1 as eluant), and the resulting product was analyzed by enantioselective HPLC and identical to the sample prepared above by chiral HPLC resolution of 14g.

2-Fluoro-4,5-dimethoxy-benzenesulfonyl chloride (34). To a suspension of sulfur trioxide/DMF complex (4.108 g, 22.4 mmol) in 1,2-dichloroethane (10 mL) was added 4-fluoroveratrole (3.49 g, 26.8 mmol) dropwise. The mixture was slowly heated to 85 °C in an oil bath, and heating was continued for 7 h. The oil bath was removed, and thionyl chloride (1.95 mL, 32 mmol) was added dropwise. The mixture was heated 4 h at 85 °C and allowed to cool to room temperature. The solution was poured into water and extracted with dichloromethane. The combined organic phases were washed with water, dried over magnesium sulfate, and evaporated to afford the product as an off-white solid (5.5 g, 96%) which was used without further purification. ^{1}H NMR (400 MHz, CDCl$_3$) δ 3.93 (s, 3H); 3.97 (s, 3H); 7.31 (d, J = 6 Hz, 1H); 7.79 (d, J = 11 Hz, 1H). MS m/e 254.0 (M)$^+$.

4-(2-Fluoro-4,5-dimethoxy-benzenesulfonyl)-morpholine. To a solution of 2-fluoro-4,5-dimethoxy-benzenesulfonyl chloride 34 (5.3 g, 20.8 mmol) in dichloromethane (30 mL) was added morpholine (3.81 mL, 43.7 mmol) dropwise. The mixture was stirred overnight at room temperature, filtered through a pad of silica gel, and eluted with ethyl acetate. The solvent was evaporated under reduced pressure to afford the product as a pale-yellow solid (5.99 g, 94%) which was used without further purification. A small sample was purified by column chromatography on silica gel (10 g, heptane/ethyl acetate 1:1 as eluant) to afford the product as a colorless solid. ^{1}H NMR (400 MHz, CDCl$_3$) δ 3.16 (m, 4H); 3.75 (m,4H); 3.90 (s, 3H); 3.94 (s, 3H); 6.73 (d, J = 11 Hz, 1H); 7.21 (d, J = 6 Hz, 1H). MS m/e 305.1 (M)$^+$.

4-Fluoro-5-(morpholine-4-sulfonyl)-benzene-1,2-diol (35). To a cooled (ice bath) solution of 4-(2-fluoro-4,5-dimethoxy-benzenesulfonyl)-morpholine (5.1 g, 16.7 mmol) in dichloromethane (100 mL) was added boron tribromide (1 M in dichloromethane, 50 mL, 50 mmol) dropwise over 30 min, and the mixture was stirred overnight at room temperature. The brown solution was slowly added to 1 M aqueous KH$_2$PO$_4$ (200 mL), and the mixture was stirred 1 h at room temperature. The phases were separated, and the aqueous phase was extracted with ethyl acetate. The combined organic phases were washed with brine, dried over magnesium sulfate, and evaporated. The resulting brown oil was purified by column chromatography on silica gel (dichloromethane/ethanol/acetic acid 18:1:0.1−10:1:0.1 as eluant) to afford the product as a light-brown oil (3.55 g, 76%) which solidified upon standing in the refrigerator. ^{1}H NMR (400 MHz, DMSO-d_6) δ 2.93 (m, 4H); 3.62 (m, 4H); 6.76 (d, J = 12 Hz, 1H); 7.04 (d, J = 7 Hz, 1H); 9.7 (br s, 1H); 10.5 (br s, 1H). MS m/e 276.0 (M − H)$^-$.

4-[2-(2,4-Dichloro-phenyl)-6-fluoro-2-(4-fluoro-phenyl)-benzo[1,3]dioxole-5-sulfonyl]-morpholine (15a). A mixture of 4-fluoro-5-(morpholine-4-sulfonyl)-benzene-1,2-diol 35 (225 mg, 0.81 mmol) and 2,4-dichloro-1-[dichloro-(4-fluoro-phenyl)-methyl]-benzene 18b (329 mg, 1.01 mmol) was heated 20 min at 180 °C

under a stream of nitrogen. The resulting brown mixture was purified by column chromatography on silica gel (heptane/ethyl acetate 3:1 as eluant) to afford the product as an off-white foam (374 mg, 87%). ^{1}H NMR (400 MHz, CDCl$_3$) δ 3.16 (m, 4H); 3.74 (m, 4H); 6.80 (d, J = 9 Hz, 1H); 7.07−7.11 (m, 2H); 7.30−7.35 (m, 2H); 7.40−7.46 (m, 3H); 7.71 (d, J = 8 Hz, 1H). MS m/e 528.1 (M+H)$^+$. Anal. ($C_{23}H_{17}F_2Cl_2NO_5S$) C, H, N, O, F, Cl, S. HRMS $C_{23}H_{17}Cl_2F_2NO_5S$: 528.02479 (M + H$^+$).

In Vivo Assays. LYSA. Samples were prepared in duplicate from 10 mM DMSO stock solutions. After evaporation (1 h) of DMSO with a centrifugal vacuum evaporator (Genevac Technologies), the compounds were dissolved in 50 mM phosphate buffer (pH 6.5), stirred for 1 h, and shaken 2 h. After one night, the solutions were filtered by using a microtiter filter plate (Millipore MSDV N65), and the filtrate and its 1/10 dilution were analyzed by direct UV measurement or by HPLC-UV. In addition, a four-point calibration curve was prepared from the 10 mM stock solutions and used for the solubility determination of the compounds. The results are expressed in μg/mL. Starting from a 10 mM stock solution, the measurement range for MW 500 was 0−666 μg/mL. In the case where the percentage of sample measured in solution after evaporation divided by the calculated maximum of sample amount was larger than 80%, the solubility was reported as larger than this value.

Solubility in Simulated Intestinal Fluids. Approximately 1−2 mg of each compound was added in excess into about 300 mL of 50 mM buffer (either Fassif or Fessif buffer) at room temperature. Composition of Fassif buffer: pH 6.5; KH$_2$PO$_4$, 3.9 g/L; KCl, 7.7 g/L; sodium taurocholate, 1.6 g/L; lecithin, 0.6 g/L. Composition of Fessif buffer: pH 5.0; acetic acid, 8.64 g/L; KCl, 15.2 g/L; sodium taurocholate, 8.08 g/L; lecithin, 2.92 g/L. Each sample was placed in a microanalysis tube, sonicated 1 h, and agitated 2 h. All suspensions were left overnight. The following day, pH was measured with a pH-meter, and the samples were filtered with a micronic filterplate (MSGVN2250) to separate any solid material from the solution. All solutions were analyzed by HPLC. The calibration line was established from five different dilutions of the compound in a DMSO stock solution (concentration approximately 1 mg/mL). From this regression equation, the solubility of the compound was determined. In cases where the drug was completely dissolved in the buffer, the value for equilibrium solubility was assumed to be higher than the value determined by HPLC and reported as such.

Rat and Human Microsomal Clearances. Human or rat microsome incubations were conducted by an automated procedure implemented on a Genesis workstation (Tecan, Switzerland). Compounds (2 μM) were incubated in microsomes at 0.5 mg protein per mL in a 50 mM potassium phosphate buffer, pH 7.4, at 37 °C. Cofactor (reduced nicotinamide adenine dinucleotide phosphate, NADPH) was produced by a generating system (glucose-6-phosphate 3.2 mM, β-nicotinamide adenine dinucleotide phosphate 2.6 mM, MgCl$_2$ 6.5 mM). Addition of the NADPH generating system to the prewarmed microsomes containing the test compound started the reaction. Aliquots (50 μL) were taken at six defined time points within 30 min and transferred into 100 μL of methanol containing an internal standard. Concentration of each compound was analyzed by LC-MS/MS by using a Synergy-4-Polar RP 18 column (Phenomenex, Torrance, CA). Quantitative detection was achieved on a SCIEX 2000 instrument (MDS Sciex, Concord, ON, Canada) by using electron spray ionization. Concentrations were determined by the ratio of test-compound and internal-standard peaks and given as a percentage of the concentration measured at the first time point (substrate depletion). Intrinsic clearance (CL$_{int}$, in μL min^{-1} mg^{-1} microsomal protein) is the rate constant of the first-order decay of the test compound, normalized for the protein concentration in the incubation. Two values were calculated to normalize this measured intrinsic clearance to an allometric scale:

hepatic clearance = (hepatic blood flow × CL$_{int}$ × protein concentration in microsome incubation × liver weight per kg body weight)/(hepatic blood flow + CL$_{int}$ × protein concentration in microsome incubation × liver weight per kg body weight)

MAB $= 100 \times (1 - (\text{hepatic clearance/hepatic blood flow}))$

(R)-14g Counterscreening. **(R)-14g** counterscreening on a panel of 67 receptors, enzymes, and channels was done by Cerep Laboratories (Le bois l'Eveque, F-86 600 Celle L'Evescault, France) at a maximal concentration of 10 μM (see Supporting Information).

In Vivo Assays. Hypothermia Assay in NMRI Mice. Animal. Male NMRI mice were used in this study and were obtained from Research Consulting Company Ltd. of Füllinsdorf (Switzerland). A total of 64 mice, weighing 29−32 g, were used in this study. Ambient temperature was 20−21 °C, and relative humidity was 55−65%. A 12-h light−dark cycle was maintained in the rooms with all tests being performed during the light phase. Access to tap water and food was ad libitum.

Method. During the experimental sessions, the mice were housed in groups of eight. All measurements were made between 12:00 a.m. and 5:00 pm. The mice were brought into this environment and habituated for at least 2 h before the start of the experiment. For each dose, eight mice were used. Rectal temperature measurements were recorded by mean of a rectal probe (RET2 of Physitemp) and digital thermometer (Digi-sense K92001517, Cole Parmer, Chicago, IL). The probe was inserted about 3.5 cm in each mouse.

Body temperature was measured:
- 20 min before administration of either vehicle or tested substance.
- Immediately before the injection of either vehicle or CP 55940.
- 20 min after administration of either vehicle or CP 55940.

Either vehicle or tested substance was administered 90 min before the injection of either vehicle or CP 55940 (0.3 mg/kg, iv).

Drugs. Tested substances and CP 55940 (Tocris Cookson, catalogue no. 0949, batch no. 6/23039) were dissolved in 0.3% Tween 80. The specific volume of administration was 10 mL/kg.

DIO Model. Animal. A group of 3-week old Sprague−Dawley rats (Iffa Credo/Charles River, France), with homogeneous body-weight values, was fed either with HFD (KLIBA 2157, 43% of energy, 19% fat, $n = 90$) or with a chow diet ($n = 10$). The chow-diet group of rats was kept as control. During the growing period, body weight was measured at the beginning of the high-fat feeding and before the randomization. After a period of 10 weeks, obese rats (high responders) were selected. High responders corresponded to rats for which the difference between their average body weight and that of chow-diet rats was at least 2 times the standard deviation of the animals from the chow-diet group [body weight (obese) − body weight (chow) > 2 SD (chow)].

Method. Homogenous groups of obese animals ($n = 9$ per group) were constituted according to the body-weight-increase values during the growing period. After 3 days of gavage adaptation, the rats received a daily dose of compounds per gavage at 5:00 p.m. During the 2-week treatment, body weight and food intake were measured daily. The total body fat mass and the lean mass content were measured in the MRI laboratory before and at the end of the treatment.

Drug. Test substances were dissolved in water with 7.5% of gelatine and 0.62% of sodium chloride. The specific volume of administration was 2 mL/kg.

Note Added after ASAP Publication. This manuscript was released ASAP on March 13, 2008 with errors in Table 1. The correct version was posted on April 3, 2008.

Supporting Information Available: Table of elemental analysis data applied to target compounds. Synthesis description for compounds **10**, **11a-b**, **12a−c**, **13**, **14a−l**, **15a−c**, **16**, and **17a−d** and their intermediates, together with spectroscopic data. Details on the panel of receptors, enzymes, and channels selected for **(R)-14g** counterscreening. Description of the lipophilicity assay and the CB1R binding and functional assays. This material is available free of charge via the Internet at http://pubs.acs.org.

References

(1) Carek, P. J.; Dickerson, L. M. Current concepts in the pharmacological management of obesity. *Drugs* **1999**, *57*, 883–904.

(2) Spanswick, D.; Lee, K. Emerging antiobesity drugs. *Expert Opin. Emerging Drugs* **2003**, *8*, 217–237.

(3) Olshansky, S. J.; Passaro, D. J.; Hershow, R. C.; Layden, J.; Carnes, B. A.; Brody, J.; Hayflick, L.; Butler, R. N.; Allison, D. B.; Ludwig, D. S. A potential decline in life expectancy in the United States in the 21st century. *N. Engl. J. Med.* **2005**, *352*, 1138–1145.

(4) Center for Disease Control and Prevention; U.S. Department of Health and Human Services (http://www.cdc.gov/).

(5) Mokdad, A. H.; Ford, E. S.; Bowman, B. A.; Dietz, W. H.; Vinicor, F.; Bales, V. S.; Marks, J. S. Prevalence of obesity, diabetes, and obesity-related health risk factors. *J. Am. Med. Assoc.* **2003**, *289*, 76–79.

(6) Kordik, C. P.; Reitz, A. B. Pharmacological treatment of obesity: Therapeutic strategies. *J. Med. Chem.* **1999**, *42*, 181–201.

(7) Das, S. K.; Chakrabarti, R. Antiobesity therapy: Emerging drugs and targets. *Curr. Med. Chem.* **2006**, *13*, 1429–1460.

(8) Tart, C. T. Marijuana intoxication: Common experiences. *Nature* **1970**, *226*, 701–704.

(9) Kirkham, T. C.; Williams, C. M.; Fezza, F. Endocannabinoid levels in rat limbic forebrain and hypothalamus in relation to fasting, feeding and satiation: Stimulation of eating by 2-arachidonoyl glycerol. *Br. J. Pharmacol.* **2002**, *136*, 550–557.

(10) Milano, W. C.; Wild, K. D.; Hui, Y. Z. PCP, THC, ethanol, and morphine and comsumption of palatable solutions. *Pharmacol., Biochem. Behav.* **1988**, *31*, 893–897.

(11) Ravinet Trillou, C.; Delgorge, C.; Menet, C.; Arnone, M.; Soubrie, P. CB1 cannabinoid receptor knockout in mice leads to leanness, resistance to diet-induce obesity and enhanced leptin sensitivity. *Int. J. Obes. Relat. Metab. Disord.* **2004**, *28*, 640–648.

(12) Pertwee, R. G. The pharmacology of cannabinoid receptors and their ligands: An overview. *Int. J. Obes.* **2006**, *30*, S13–S18.

(13) Gadde, K. M.; Allison, D. B. Cannabinoid-1 receptor antagonist, rimonabant, for management of obesity and related risks. *Circulation* **2006**, *114*, 974–984.

(14) Van Gaal, L.; Rissanen, A.; Scheen, A.; Ziegler, O.; Rössner, S. Effects of the cannabinoid-1 receptor blocker rimonabant on weight reduction and cardiovascular risk factors in overweight patients: 1-Year experience from the RIO-Europe study. *Lancet* **2005**, *365*, 1389–1397.

(15) Lange, J. H. M.; Coolen, H. K. A. C.; Van Stuivenberg, H. H.; Dijksman, J. A. R.; Herremans, A. H. J.; Ronken, E.; Keizer, H. G.; Tipker, K.; McCreary, A. C.; Veerman, W.; Wals, H. C.; Stork, B.; Verveer, P. C.; Den Hartog, A. P.; De Jong, N. M. J.; Adolfs, T. J. P.; Hoogendoorn, J.; Kruse, C. G. Synthesis, biological properties, and molecular modeling investigations of novel 3,4-diarylpyrazolines as potent and selective CB1 cannabinoid receptor antagonists. *J. Med. Chem.* **2004**, *47*, 627–643.

(16) Lin, L. S.; Lanza, T. J., Jr.; Jewell, J. P.; Liu, P.; Shah, S. K.; Qi, H.; Tong, X.; Wang, J.; Xu, S. S.; Fong, T. M.; Shen, C.-P.; Lao, J.; Xiao, J. C.; Shearman, L. P.; Stribling, D. S.; Rosko, K.; Strack, A.; Marsh, D. J.; Feng, Y.; Kumar, S.; Samuel, K.; Yin, W.; Van der Ploeg, L. H. T.; Goulet, M. T.; Hagmann, W. K. Discovery of N-[(1S,2S)-3-(4-chlorophenyl)-2- (3-cyanophenyl)-1-methylpropyl]-2-methyl-2-{[5-(trifluoromethyl)pyridin-2-yl]oxy}propanamide (MK-0364), a novel, acyclic cannabinoid-1 receptor inverse agonist for the treatment of obesity. *J. Med. Chem.* **2006**, *49*, 7584–7587.

(17) Fong, T. M.; Guan, X.-M.; Marsh, D. J.; Shen, C.-P.; Stribling, D. S.; Rosko, K. M.; Lao, J.; Yu, H.; Feng, Y.; Xiao, J. C.; Van der Ploeg, L. H. T.; Goulet, M. T.; Hagmann, W. K.; Lin, L. S.; Lanza, T. J., Jr.; Jewell, J. P.; Liu, P.; Shah, S. K.; Qi, H.; Tong, X.; Wang, J.; Xu, S. S.; Francis, B.; Strack, A. M.; MacIntyre, D. E.; Shearman, L. P. Antiobesity efficacy of a novel cannabinoid-1 receptor inverse agonist, N-[(1S,2S)-3-(4-chlorophenyl)-2-(3-cyanophenyl)-1-methylpropyl]-2-methyl-2-{[5-(trifluoromethyl)pyridin-2-yl]oxy}propanamide (MK-0364), in rodents. *J. Pharmacol. Exp. Ther.* **2007**, *321*, 1013–1022.

(18) Vemuri, V. K.; Janero, D. R.; Makriyannis, A. Pharmacotherapeutic targeting of the endocannabinoid signaling system: Drugs for obesity and the metabolic syndrome. Physiol. Behav, in press, doi:10.1016/j.psysbeh.2007.11.012.

(19) Sanofi-Aventis Press Release, June 13, 2007 and June 29, 2007.

(20) Bengtsson, S.; Hoegberg, T. Secondary β-aminobenzamide and heteroatom directed lithiation in the synthesis of 5,6-dimethoxyanthranilamides and related compounds. *J. Org. Chem.* **1989**, *54*, 4549–4553.

(21) Angehrn, P.; Furlenmeier, A.; Hebeisen, P.; Hofheinz, W.; Link, H. Preparation of (heterocyclylthio)desacetyloxycephalosporinates as antibiotics. Eur. Pat. Appl. EP544166A2,1993.

(22) Goetschi, E. Preparation of alkoxyiminocephalosporin derivatives as antibiotics and pharmaceutical compositions containing them. Eur. Pat. Appl. EP303172A2, 1989.

(23) Alanine, A.; Bleicher, K.; Guba, W.; Haap, W.; Kuber, D.; Luebbers, T.; Plancher, J.-M.; Rogers-Evans, M.; Schneider, G.; Zuegge, J.; Roche, O. Preparation of benzodioxoles as CB1 receptor modulators for potential therapeutic use against obesity and other disorders. PCT Int. Appl. WO 2004013120 A1, 2004.

(24) Raabe, D.; Hoerhold, H. H. Trichloromethylation of benzene with carbon tetrachloride. *J. Prakt. Chem.* **1987**, *329*, 1131–1132.

(25) Hare, L. E.; Lu, M. C.; Sullivan, C. B.; Sullivan, P. T.; Counsell, R. E.; Weinhold, P. A. Aromatic amino acid hydroxylase inhibitors. 3. In vitro inhibition by azadopamine analogs. *J. Med. Chem.* **1974**, *17*, 1–5.

(26) Mochida, K.; Ono, Y.; Yamasaki, M.; Shiraki, C.; Hirata, T.; Sato, K.; Okachi, R. Aminothiazolylglycyl derivatives of carbacephem antibiotics. II. Synthesis and antibacterial activity of novel aminothiazolyl cephem compounds with hydroxypyridone moiety. *J. Antibiot.* **1987**, *40*, 182–189.

(27) Tao, E. V. P.; Miller, W. D. Synthesis of bicyclic aromatic sulfonic acids, sulfonyl chlorides, and sulfonamides. Eur. Pat. Appl. EP 583960A2, 1994.

(28) Padwa, A.; Dimitroff, M.; Waterson, A. G.; Wu, T. IMDAF cycloaddition as a method for the preparation of pyrrolophenanthridine alkaloids. *J. Org. Chem.* **1998**, *63*, 3986–3997.

(29) Schneider, G.; Clement-Chomienne, O.; Hilfiger, L.; Schneider, P.; Kirsch, S.; Böhm, H.-J.; Neidhardt, W. Virtual screening for bioactive molecules by evolutionary de novo design. *Angew. Chem., Int. Ed. Engl.* **2000**, *39*, 4130–4133.

(30) Schneider, G.; Lee, M.-L.; Stahl, M.; Schneider, Pe. De novo design of molecular architectures by evolutionary assembly of drug-derived building blocks. *J. Comput. Aided. Mol. Des.* **2000**, *14*, 487–494.

(31) Lainton, J. A. H.; Huffman, J. W.; Martin, B. R.; Compton, D. R. 1-Alkyl-3-(1-naphthoyl)pyrroles: A new class of cannabinoid. *Tetrahedron Lett.* **1995**, *36*, 1401–1404.

(32) Rogers-Evans, M.; Alanine, A.; Bleicher, K.; Kube, D.; Schneider, G. Identification of novel cannabinoid receptor ligands via evolutionary de novo design and rapid parallel synthesis. *QSAR Comb. Sci.* **2004**, *26*, 426–430.

(33) Greene, T. W.; Wuts, P. G. M. *Protective Groups in organic Synthesis*, 3rd ed.; Wiley: New York, 1999; pp 289–290..

(34) Nava, F.; Carta, G.; Gessa, G. L. Permissive role of dopamine D(2) receptors in the hypothermia induced by delta(9)-tetrahydrocannabinol in rats. *Pharmacol., Biochem. Behav.* **2000**, *66*, 183–187.

(35) Frei, B.; Plancher, J.-M.; Roever, S.; Zimmerli, D. Preparation of [6-fluorobenzo[1,3]dioxolyl] morpholin-4-ylmethanones as cannabinoid CB1 receptor ligands. PCT Int. Appl. WO 2006136502 A1, 2006.

(36) Alsenz, J.; Haenel, E. Development of a 7-day, 96-well Caco-2 permeability assay with high-throughput direct UV compound analysis. *Pharm. Res.* **2003**, *20*, 1961–1969.

(37) Plancher, J.-M.; Taylor, S. Preparation of spirobenzodioxole-dibenzocycloheptenecarbonylpiperidines and -morpholines as cannabinoid CB1 receptor antagonists/inverse agonists. U.S. Pat. Appl. US 2005165012 A1, 2005.

(38) Plancher, J.-M.; Taylor, S. Preparation of spirobenzodioxole-dibenzocycloheptenylcarbonylmorpholines as cannabinoid CB1 receptor antagonists. U.S. Pat. Appl. Publ. US 2006100206 A1, 2006.